



PDLC-based VOA with a small polarization dependent loss

Kuan Ming Chen, Hongwen Ren, Shin Tson Wu*

College of Optics and Photonics, University of Central Florida, Orlando, FL 32816-2700, United States

ARTICLE INFO

Article history:

Received 29 April 2009

Received in revised form 7 August 2009

Accepted 10 August 2009

ABSTRACT

A polymer-dispersed liquid crystal (PDLC)-based variable optical attenuator (VOA) was demonstrated to exhibit a relatively small polarization dependent loss (PDL) in the optical communication C band. The influence of the PDLC characteristics, the temperature, as well as the wavelength of the laser irradiation, on the PDLC VOA performance was analyzed. The PDL, the insertion loss at saturated voltage, and the operating voltage of the PDLC-based VOA were reduced by optimizing the fabrication conditions and applying a bias voltage to the PDLC cells during polymerization-induced phase separation.

© 2009 Elsevier B.V. All rights reserved.

1. Introduction

Variable optical attenuator (VOA) based on polymer-dispersed liquid crystal (PDLC) has been studied extensively in recent years. PDLC is a composite material in which liquid crystal droplets are randomly distributed in polymer matrix [1–5]. For VOA applications, the following four criteria are highly desirable: high dynamic range, small polarization dependent loss (PDL), low insertion loss in the voltage-on state, and low operating voltage. A PDLC-based VOA with a 15 dB optical attenuation at the operating wavelength $\lambda = 1.3 \mu\text{m}$ is demonstrated [2]. However, it is difficult to achieve a high optical attenuation while keeping a low polarization dependent loss (PDL) under the same preparation conditions [3]. So far, only handful research efforts have addressed the abovementioned four requirements [5]. To improve the PDLC VOA performances, the phase separation morphology plays a crucial role and should be optimized.

In this paper, we report an improved method for enhancing the PDLC VOA performances. We first prepared several PDLC cells under different UV curing conditions. Once the optimal curing condition is obtained, we applied a bias voltage to the PDLC cell during UV exposure stage. As a result, our VOA exhibits a smaller PDL and insertion loss than the regularly prepared one, although the dynamic range is slightly reduced. Detailed cell fabrication conditions and device performances are described.

2. Sample preparation

To prepare PDLC samples, we mixed Merck nematic LC mixture BL-036 and UV curable prepolymer NOA65 at 70:30 wt.% ratios. The refractive index of the uncured NOA65 is $n = 1.5149$ at $\lambda = 1.55 \mu\text{m}$ [6]. Regarding to BL-036, we measured its refractive

indices using an Abbe refractometer (Atago, DR-M4) at six visible wavelengths and then extrapolated its refractive index to $1.55 \mu\text{m}$. The extrapolated results are $n_o = 1.5104$ and $\Delta n = 0.2617$ at $\lambda = 1.55 \mu\text{m}$. The mixture was stirred thoroughly in an isotropic state and then injected into empty cells by capillary action. The inner surfaces of the glass substrates were coated with ITO (indium tin oxide) electrode. The temperature of the cell was controlled using a hot plate. An UV lamp (Model 98016, LOCTITE) was used as the curing light source. To find the optimal curing conditions, we cured the PDLC cells at different temperatures while keeping the UV exposure time at 4 min for each sample. The UV intensity was controlled at $\sim 180 \text{ mW/cm}^2$ during curing process. After UV curing, the cells were cooled to room temperature for several hours until polymerization process was complete. When the morphology was stabilized, the cells were ready for characterizations.

Fig. 1 shows the experimental setup for characterizing the PDLC devices. A tunable laser light source (ANDO AQ4321D, $\lambda = 1.52\text{--}1.62 \mu\text{m}$) was employed. A manual polarization controller (FPC560, Thorlabs) was used to change the polarization state of the input light. The optical beam coming from a single-mode fiber was collimated by the gradient refractive index (GRIN) rod lens. The collimated beam propagated to the GRIN lens and impinged the connected single-mode optical fiber. The output beam was monitored by an optical power meter (ANDO AQ8201-21). The PDLC sample was placed between the two GRIN lenses in free space. The distance of the two lenses was fixed at 4 cm.

3. Results and discussions

Usually, the dynamic extinction ratio (also called dynamic range) of a PDLC is related to the LC droplet size, cell thickness, and LC birefringence [7]. To obtain a maximum dynamic range, the optimum LC droplet radius (a_{opt}), LC birefringence (Δn), and operating wavelength (λ) should satisfy following relationship [9]:

* Corresponding author. Tel.: +1 407 823 4763; fax: +1 407 823 6880.
E-mail address: swu@mail.ucf.edu (S.T. Wu).

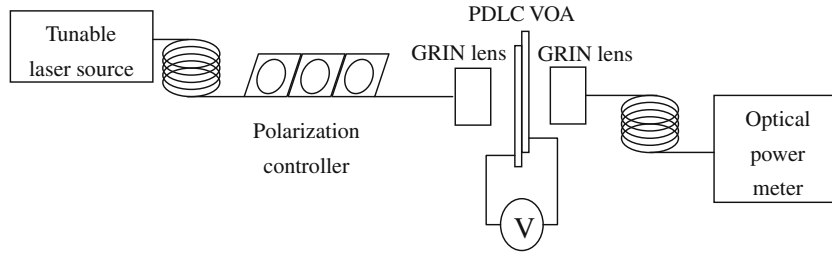


Fig. 1. Experimental setup for measuring PDLC-based VOA performances.

$$a_{opt} = \frac{0.3}{\Delta n} \lambda \quad (1)$$

As mentioned above, BL-036 has $\Delta n \sim 0.267$ at $\lambda = 589$ nm. As the wavelength increases, the LC birefringence decreases and saturates to a plateau [8,10,11]. At $\lambda = 1550$ nm, $\Delta n \sim 0.26$. Plugging these two numbers into Eq. (1), we find the LC droplet diameter is ~ 3.6 μm .

Due to the bipolar or axial orientation of LC in the droplet cavities, a thin (~ 15 μm) PDLC layer will cover only four droplets along the cell gap direction. Because each LC droplet has a preferred orientation axis, for large LC droplets confined in a thin cell gap it is difficult to get symmetric orientation distribution of the droplet axes along substrate surface. In a thick cell, the number of droplets is large and the averaged effective index is about the same in all polarization directions. In a thin cell, the number of LC droplets is limited and, moreover, LC droplets with overlaid orientation along substrate surface will cause the incident light to see a large birefringence as it passing through the PDLC. Therefore, a PDLC with such LC droplets usually processes a large PDL. Increasing cell gap helps to suppress the PDL, because the symmetric probability of the LC droplet orientation along substrate surface increases. However, the operating voltage will increase significantly.

To prepare PDLC for VOA, both dynamic range and PDL should be taken into consideration at the same time. To optimize the PDLC performances, we first find the optimum fabrication condition and then apply a voltage to control the LC droplet orientation during polymerization-induced phase separation. Our results show that the PDL is decreased dramatically in the voltage-off state and the dynamic range is still in the acceptable level.

Fig. 2 shows the voltage dependent dynamic range and PDL of the PDLC samples under different curing temperatures. The thickness of each PDLC cell is controlled to be ~ 15 μm . The operating voltage is an ac square wave signal (1 kHz). For the PDLC sample cured at 72 °C, the dynamic range is ~ 11 dB at $V = 0$. As the applied voltage increases, the dynamic range decreases. At $\sim 65 V_{\text{rms}}$, the insertion loss is ~ 0.8 dB and the response time was measured to be ~ 80 ms. The response time of a PDLC cell depends on the droplet size, shape, LC rotational viscosity, and applied voltage [12]. Because of the relatively large droplet diameter (~ 4 μm), the response time is slower than that used for visible display devices where the droplet size is around 1–2 μm .

Also included in Fig. 2 is the measured PDL. At $V = 0$, the PDL is over 1 dB. As the applied voltage increases, the PDL decreases correspondingly. This is due to most LC droplets are enforced to orient along the electric fields, and thus decrease the non-symmetrical orientation. PDLC with such a larger PDL is not useful for optical fiber controller applications. PDLCs cured at other temperatures present either a large insertion loss at high voltage or low optical switch. Such results mean the PDLC performances are sensitive to the curing temperature. Therefore, we optimized PDLC performances by curing them at 72 °C.

To optimize PDLC performances, several PDLC samples with different cell gaps were prepared at the same cure temperature

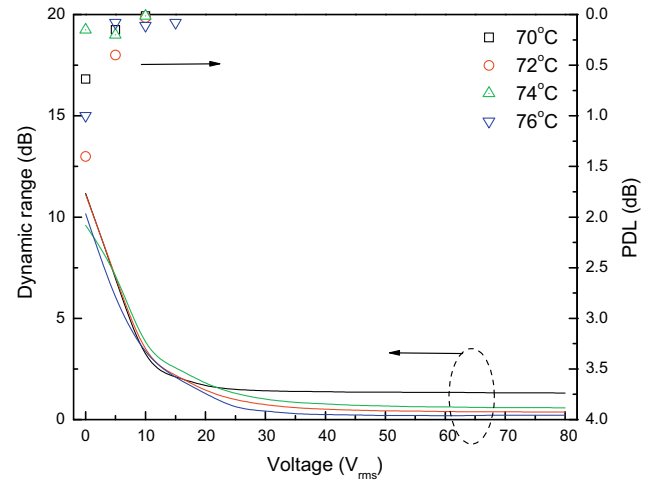


Fig. 2. Performances of PDLC samples prepared at different curing temperatures. Black curve stands for the dynamic range of sample cured at 70 °C; red curve at 72 °C; green curve at 74 °C; blue curve at 76 °C. black square dots stand for PDL of sample cured at 70 °C; red circles at 72 °C; green upward triangles at 74 °C; blue downward triangles at 76 °C. (For interpretation of the references to colour in this figure legend, the reader is referred to the web version of this article.)

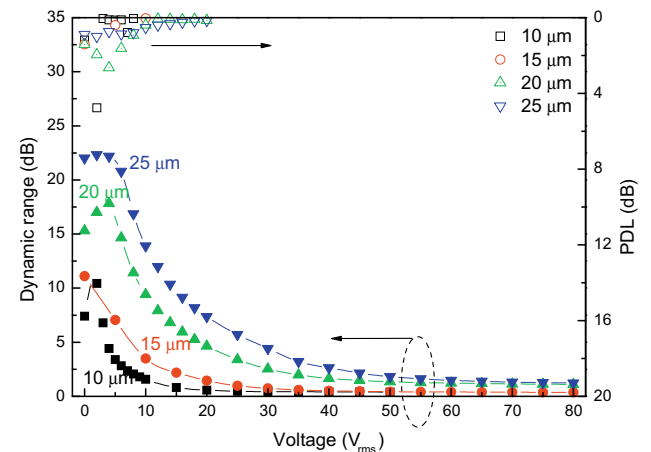


Fig. 3. Voltage dependent dynamic range and PDL of PDLC cells with different thickness cured at 72 °C.

(72 °C). Fig. 3 depicts the voltage dependent dynamic range and PDL of the PDLC samples. For a PDLC cell with thickness of ~ 25 μm , the dynamic extinction ratio is ~ 20 dB and the PDL is ~ 1 dB at $V = 0$. However, the insertion loss is over 1 dB even at 80 V_{rms} . By comparison with other PDLCs, the PDLC with 15 μm still presents reasonable performances except the larger PDL at $V = 0$.

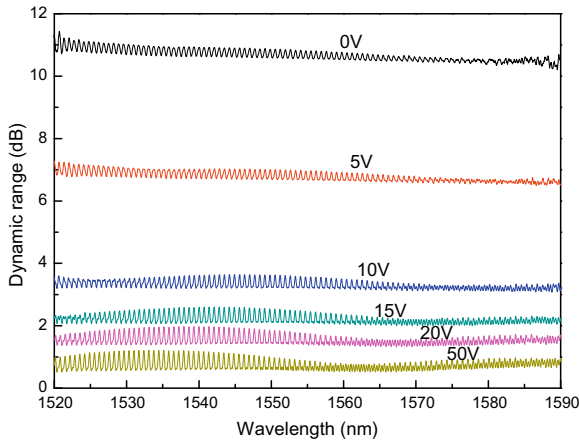


Fig. 4. Dispersion of the voltage dependent dynamic range of the PDLC VOAs.

The dynamic range of a PDLC is dependent on the LC droplet size and the wavelength [13]. If LC droplet size is too small or too large as compared to the operating wavelength, then the light scattering capability of PDLC will decrease so that the dynamic range will decrease largely [14]. Fig. 4 shows the dispersion spectra of the 15- μm -thick PDLC cell in the spectral range from 1520 to 1570 nm (C band). The dynamic range at a given voltage is quite inert to the operating wavelength in this range. The small oscillations of each curve come from the interference of the two ITO surfaces of the PDLC cell. At $V = 0$, the dynamic range is ~ 11 dB. As the voltage increases, dynamic range decreases gradually, and finally reaches 0.5 dB at $V = 50 V_{\text{rms}}$. From Fig. 4, we find that in the C band the PDLC-based VOA at a given voltage is wavelength independent. However, the dynamic range of our VOA is still not as large as expected. This result suggests that the LC droplet size distribution is a little wide.

As observed from Fig. 3, the PDL of the PDLC cells we fabricated is still too large. To suppress PDL, we applied an external voltage to the cell during polymerization-induced phase separation. The sample fabrication process is the same as that of the abovementioned

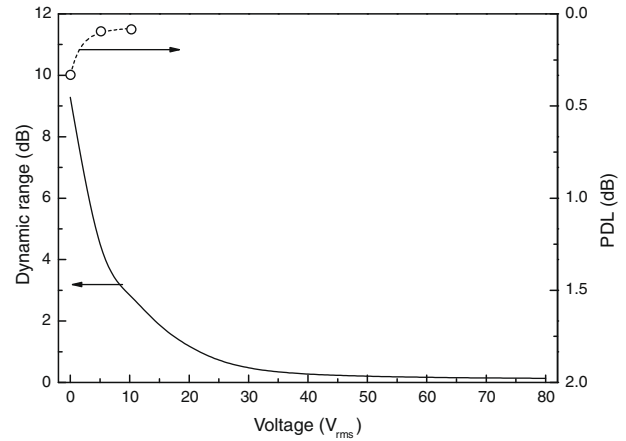


Fig. 5. Voltage dependent dynamic range and PDL of the biased sample (15 μm) cured at 72 $^{\circ}\text{C}$. The black line presents the voltage dependent dynamic range and the empty circles present the voltage dependent PDL.

PDLC cells. First we injected the mixture into a 15- μm empty cell and the cell temperature was controlled at ~ 72 $^{\circ}\text{C}$, then a voltage with $50 V_{\text{rms}}$ (1 kHz square waves) was applied to the cell for the whole UV curing process. The cell was then exposed to UV light for 4 min. Fig. 5 shows the dynamic range and PDL of the prepared PDLC cell. It shows the dynamic range decreases from ~ 11 to ~ 9.5 dB, but the PDL is greatly suppressed. At $V = 0$, the PDL is ~ 0.32 dB as compared to ~ 1 dB for a sample prepared without any biased voltage. At the saturated voltage ($50 V_{\text{rms}}$), the insertion loss is ~ 0.5 dB.

Fig. 6a and b depicts the schematic LC director's distribution of PDLC cells fabricated without and with a biased voltage. Fig. 6c and d are the PDLC morphology pictures of the unbiased and the biased cells observed under a cross polarized optical microscope, respectively. Without a bias voltage, as Fig. 6c shows, the LC droplets in the voltage-off state are randomly oriented and the LC droplet sizes are fairly large. From Fig. 6c and d, the size of the droplets is esti-

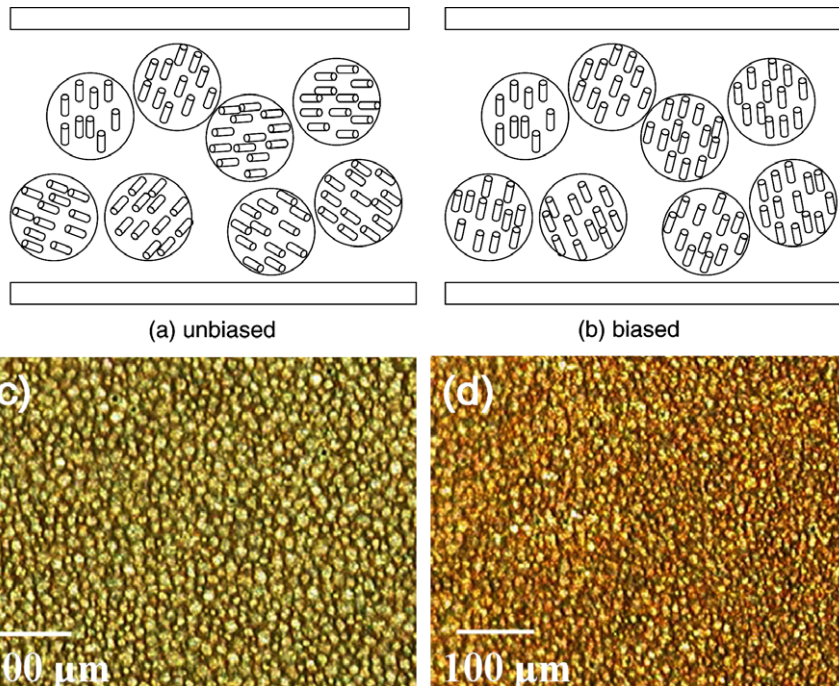


Fig. 6. Schematics of LC droplet orientations in PDLC with (a) unbiased and (b) biased voltage during UV exposure. PDLC (15 μm thick) morphology pictures under cross polarized microscope of (c) unbiased and (d) biased cases.

mated to range from ~ 3 to ~ 10 μm in the 15- μm cell gap. Within a 100×100 μm^2 area the average droplet size in Fig. 6c is ~ 7.8 μm , with a standard deviation of 4.0 μm ; and the average droplet size in Fig. 6c is 5.2 μm , with a standard deviation of 2.1 μm . When a laser beam traverses the PDLC cell, the beam will see a large non-symmetric LC orientation. As a result, the PDL is large. When a voltage is applied to the cell during the entire polymerization process, the LC molecules are forced to align along the electric field direction. The formed LC droplets present the same preferred orientation along electric field. When the external electric field is removed, the orientation of the LC droplets deviates from the electric field direction due to the anchoring effect of their cavity interface. After balance, most of LC droplets have a preferred orientation toward the same direction [15,16], as shown in Fig. 6b. Due to the more uniform LC orientation, the PDL decreases. The trade-off of using this method is the slightly reduced dynamic range. To overcome this problem, we could use a high birefringence LC [17,18], or increase the cell gap. The former approach is more favorable because increasing cell gap would lead to an increased operating voltage.

4. Conclusion

Various PDLC samples were prepared for optical fiber VOA applications. By optimizing the fabrication conditions, our PDLC-based VOA exhibits a large dynamic range, low insertion loss, and reasonably low operating voltage. By applying an external field to the PDLC cell during UV polymerization-induced phase separation, the formed LC droplets present a pretilt orientation, thus the PDL is decreased significantly. Although this approach leads

to a slight decrease in dynamic range, this loss can be recovered by increasing the cell gap, and narrowing the LC droplet size distribution.

Acknowledgement

The authors would like to thank AFOSR for the financial support under Contract No. FA95550-09-1-0170.

References

- [1] D.E. Lucchetta, R. Karapinar, A. Manni, F. Simoni, *J. Appl. Phys.* 91 (2002) 6060.
- [2] K. Takizawa, K. Kodama, K. Kishi, *Appl. Opt.* 37 (1998) 3181.
- [3] H. Ramanitra, P. Chanclou, L. Dupont, B. Vinouze, *Opt. Eng.* 43 (2004) 1445.
- [4] T.J. Bunning, L.V. Natarajan, V.P. Tondiglia, R.L. Sutherland, *Annu. Rev. Mater. Sci.* 30 (2000) 83.
- [5] P. Chanclou, B. Vinouze, M. Roy, C. Cornu, *Opt. Commun.* 248 (2005) 167.
- [6] J. Li, G. Baird, Y.H. Lin, H. Ren, S.T. Wu, *J. Soc. Inf. Display* 13 (2005) 1017.
- [7] S.T. Wu, D.K. Yang, *Reflective Liquid Crystal Displays*, Wiley, Chichester, 2001.
- [8] S.T. Wu, *Phys. Rev. A* 33 (1986) 1270.
- [9] D. Bosc, C. Trubert, B. Vinouze, M. Guilbert, *Appl. Phys. Lett.* 68 (1996) 2489.
- [10] S.T. Wu, U. Efron, L.D. Hess, *Appl. Phys. Lett.* 44 (1984) 1033.
- [11] J. Li, S.T. Wu, S. Brugioni, S. Faetti, R. Meucci, *J. Appl. Phys.* 97 (2005) 073501.
- [12] B.G. Wu, J.H. Erdmann, J.W. Doane, *Liq. Cryst.* 5 (1989) 1453.
- [13] S. Zumer, *Phys. Rev. A* 37 (1988) 4006.
- [14] Y.H. Lin, H. Ren, S.T. Wu, *Appl. Phys. Lett.* 84 (2004) 4083.
- [15] J.D. Margerum, A.M. Lackner, E. Ramos, K.C. Lim, W.H. Smith Jr., *Liq. Cryst.* 5 (1989) 1477.
- [16] J.D. Margerum, A.M. Lackner, J.H. Erdmann, E. Sherman, *Proc. SPIE* 1455 (1991) 27.
- [17] S. Gauza, H. Wang, C.H. Wen, S.T. Wu, A. Seed, R. Dabrowski, *Jpn. J. Appl. Phys.* 42 (2003) 3463.
- [18] S. Gauza, C.H. Wen, S.T. Wu, N. Janarthanan, C.S. Hsu, *Jpn. J. Appl. Phys.* 43 (2004) 7634.